Theoretical Modelling of Frequency Dependent Elastic Loss in Composite Piezoelectric Transducers

Leigh-Ann Orr[†], Anthony J. Mulholland[†*]

, Richard L. O'Leary[‡], Agnes Parr[‡], Richard A. Pethrick[§],

and Gordon Hayward[‡]

[†] Department of Mathematics, University of Strathclyde,

Glasgow, UK G1 1XH

[‡] The Centre for Ultrasonic Engineering,

Department of Electronic and Electrical Engineering,

University of Strathclyde, Glasgow, UK G1 1XW

[§] Department of Pure and Applied Chemistry,

University of Strathclyde, Glasgow, U.K. G1 1XL

September 21, 2007

*Address for correspondence: Department of Mathematics, University of Strathclyde, Livingstone Tower, 26 Richmond Street, Glasgow G1 1XH, U.K., Tel: ++44 (0)141 548 2971, Fax: ++44 (0)141 548 3345, email: ajm@maths.strath.ac.uk

Abstract

The large number of degrees of freedom in the design of piezoelectric transducers requires a theoretical model that is computationally efficient so that a large number of iterations can be performed in the design optimisation. The materials used are often lossy, and indeed loss can be used to enhance the operational characteristics of these designs. Motivated by these needs, this paper extends the one-dimensional Linear Systems Model to incorporate frequency dependent elastic loss. The reception sensitivity, electrical impedance and electromechanical coupling coefficient of a 1-3 composite transducer, with frequency dependent loss in the polymer filler, is investigated. By plotting these operating characteristics as a function of the volume fraction of piezoelectric ceramic an optimum design is obtained. A device with a non-standard, high shear attenuation polymer is also simulated and this leads to an increase in the electromechanical coupling coefficient. A comparison with finite element simulations is then performed. This shows that the two methods are in reasonable agreement in their electrical impedance profiles in all the cases considered. The plots are almost identical away from the main resonant peak where the frequency location of the peaks are comparable but there is in some cases a 20 percent discrepancy in the magnitude of the peak value and in its bandwidth. The finite element model also shows that the use of a high shear attenuation polymer filler damps out the unwanted, low frequency modes whilst maintaining a reasonable impedance magnitude.

Keywords: ANISOTROPIC COMPOSITES, ULTRASONIC TRANSDUCER, ELASTIC LOSS

PACS Code: 43.35.+d

1 Introduction

This objective of this paper is to extend the Linear Systems Model (LSM) of piezoelectric ultrasonic transducers by incorporating frequency dependent elastic loss. This then facilitates a discussion of high shear attenuation fillers for composite designs and also a comparison with results from a finite element model (FEM). The motivation stems from the use of such models in the rapid prototyping of these transducers and the fact that the materials used are lossy, and indeed loss can be used to enhance the operational characteristics of the design. The large number of degrees of freedom in such designs require a model that is computationally efficient so that a large number of iterations can be performed in a design optimisation. The methodology is therefore to derive and implement an LSM with elastic loss and, in order to gauge the effect that this frequency dependent loss has on the operational characteristics of composite piezoelectric transducers, present a series of model simulations. The effect that frequency dependent loss in a standard polymer filler has on the transmission sensitivity, electrical impedance and electromechanical coupling coefficient is described. An anisotropic passive phase material is also analysed, along with the effect of varying the volume fraction (i.e. the device architecture) of the ceramic phase. Finally a comparison between this approach and a Finite Element Method (FEM) is discussed.

Composite transducers composed of a piezoelectric ceramic and a passive polymer phase provide better electromechanical coupling and acoustic impedance characteristics than conventional single phase transducers [1]. For the transducer to operate efficiently it is required that the acoustic impedance of the piezoelectric component (Z_c) matches, as well as is possible, the acoustic impedance of the load medium (Z_L). A closer acoustic impedance matching with the load medium reduces internal wave reflection at the front face of the transducer. Typically the load medium has a far lower impedance than the piezoelectric ceramic and so the inclusion of a low mechanical impedance polymer in a com-

posite piezoelectric component serves to enhance the energy transfer. Ideally a single longitudinal mode in the thickness direction will drive the transducer in a piston like fashion. Other modes, propagating in other directions, can interfere with this behaviour and hence it is of interest to theoretically predict the design criteria, material parameters, etc. that will ensure a large frequency band gap between the desired thickness mode and these other waves. This will enhance the amplitude and bandwidth of the transmission and reception sensitivity.

2 Linear Systems Modelling

For thickness mode transducers, the dynamics can be approximately described by a one-dimensional model. By coupling the piezoelectric constitutive equations with the one-dimensional wave equation for the mechanical displacement, the LSM can be derived [2]. In a series of papers, the dependency of both the reception and transmission characteristics of the transducer on its physical parameters has been investigated using a systems block diagram approach [3, 4, 5]. Composite transducers are typically manufactured by slicing the piezoelectric ceramic into a bristle block of vertical pillars and then filling the inter-pillar space with a passive polymer. When the ceramic has a connectivity in only one direction whilst the polymer has connectivity in all three directions, this topology is described as 1-3. Alternatively, a 2-2 composite is made by cutting the ceramic longitudinally in only one direction so that there is connectivity in two directions for both the ceramic and polymer.

In order to utilise the LSM the effective properties of the 1-3 composite transducer must be derived. The piezoelectric constitutive equations are reduced to a one-dimensional caricature of the composite [6] and then the electrical impedance of the device (Z_T) is given by

$$Z_T = \frac{1}{pC_o}\left(1 - h_{33}^2 C_o \frac{K_F T_F + K_B T_B]}{2pZ_c}\right). \tag{1}$$

where p is the Laplace variable, $C_0 = A_r \bar{\epsilon}_{33}/L$ is the (clamped) capacitance of the

piezoelectric component of the device (L is its thickness, A_r is its cross-sectional area, $\bar{\epsilon}_{33}$ is its effective permittivity), $h_{33} = \bar{e}_{33}/\bar{\epsilon}_{33}$ is its effective piezoelectric constant, $T_F = 2Z_c/(Z_c + Z_L)$, $T_B = 2Z_c/(Z_c + Z_B)$, $K_F = ((1 - e^{-p\xi})(1 - R_B e^{-p\xi}))/(1 - R_F R_B e^{-2p\xi})$, $K_B = ((1 - e^{-p\xi})(1 - R_F e^{-p\xi}))/(1 - R_F R_B e^{-2p\xi})$, $R_F = (Z_c - Z_L)/(Z_c + Z_L)$ is the reflection coefficient at the front face of the transducer, and $R_B = (Z_c - Z_B)/(Z_c + Z_B)$ is the reflection coefficient at the back face of the transducer. The transit time of a plane wave through the piezoelectric component of the transducer is $\xi = L/v$ where the longitudinal phase velocity is $v = \sqrt{\bar{c}^D_{33}/\bar{\rho}}$, $\bar{\rho}$ is the volume averaged density, and $c^D_{33} = \bar{c}_{33} + (\bar{e}_{33})^2/\bar{\epsilon}_{33}$ is the stiffened elastic modulus. The acoustic impedance of the transducer is $Z_c = \bar{\rho} v A_r$, and the transducer has a backing material (subscript B) and (for simplicity) no matching layer; the device transmits directly into a load medium (subscript L).

The force produced at the front face of the transducer (F_F) is maximised at the electrical resonant frequency (f_e) which coincides with the first minimum in the electrical impedance plot (absolute value) when viewed as a function of frequency. The general transfer function relating the stress wave generated into the load medium to the input voltage (V_s) is the *transmission sensitivity* given by

$$\frac{F_F}{V_s} = -h_{33} a (A_F/2) Y K_F (1 - h^2_{33} Y (K_F T_F + K_B T_B)/(2pZ_c))^{-1} \qquad (2)$$

where $Y = C_0/(1 + pC_0 b)$, $b = Z_0 Z_E/(Z_0 + Z_E)$, $A_F = 2Z_L/(Z_c + Z_L)$, $a = Z_E/(Z_0 + Z_E)$, the transducer is placed in parallel with an electrical load impedance Z_E and the combination is placed in series with an electrical load impedance Z_0. A similar derivation can be performed for the reception mode to give the *reception sensitivity*; the ratio of the received voltage to the magnitude of the incident force

$$\frac{V}{F_F} = \frac{-h_{33} T_F K_F U/pZ_c}{1 - h^2_{33}(K_F T_F/2 + K_B T_B/2) U/(p^2 Z_c Z_E)}, \qquad (3)$$

where $U = pC_0 b/(1 + pC_0 b)$. When in response mode the aim is to maximize the voltage resulting from a force at the front face, and this occurs at the mechan-

ical resonant frequency (f_m). Finally, a measure of the efficiency with which the transducer converts electrical energy to mechanical energy is given by the electromechanical coupling coefficient k [2]. In equation (1) the dimensionless expression $h_{33}^2 C_0/pZ_c$, is the square of the electromechanical coupling coefficient. Since K_F, K_B, T_F and T_B are $O(1)$ then k must also be $O(1)$ so that the two additive terms in equation (1) are of similar order and resonant behaviour can then occur. For a half-wavelength active layer device this expression can be re-expressed as

$$k = \frac{\bar{e}_{33}}{\sqrt{c_{33}^D \bar{\epsilon}_{33}}}. \tag{4}$$

3 Incorporation of Elastic Loss

In this paper a frequency dependent, elastic loss mechanism is incorporated into the passive phase. To illustrate the approach, the shear modulus $G = c_{44}^s$ is considered; the Bulk and Young's moduli (Y) can be treated in a similar fashion. The elastic loss is introduced via the complex expression [7]

$$G = G' + iG'' \tag{5}$$

where

$$G' = G_r + \frac{(G_u - G_r)\omega^2\tau_G^2}{1 + \omega^2\tau_G^2}, \tag{6}$$

$$G'' = \frac{(G_u - G_r)\omega\tau_G}{1 + \omega^2\tau_G^2}, \tag{7}$$

G_r is the relaxed shear modulus, G_u is the unrelaxed shear modulus, ω is the angular frequency and τ_G is the shear relaxation time. The degree of loss can be expressed in terms of a dimensionless loss tangent $\tan\delta$ [7], or an attenuation coefficient α_G (Nepers/m)[8], where

$$\tan\delta = \frac{G''}{G'}, \tag{8}$$

and a Taylor series expansion relates the two expressions via

$$\alpha_G = \frac{\omega}{2c_G} \tan \delta, \tag{9}$$

where c_G is the (measured/real part of the) shear wave velocity. To find τ_G, G_u and G_r, the attenuation coefficient and the wave speed must be measured over a range of frequencies. Using basic calculus an expression for the frequency where $\tan \delta$ achieves its maximum (ω_{max}) can be derived. It can then be shown that

$$\tau_G = \frac{-c_G \alpha_G (\omega_I^2 + \omega_{max}^2) + \sqrt{c_G^2 \alpha_G^2 (\omega_I^2 + \omega_{max}^2)^2 + \omega_I^4 \omega_{max}^2}}{\omega_I^2 \omega_{max}^2}. \tag{10}$$

where ω_I is the particular frequency where the real part of the shear modulus ($G_I' = \rho c_G (\omega_I)^2$) is experimentally determined. Further analysis shows that

$$G_u = \frac{G_I'(2c_G \alpha_G + \omega_I^2 \tau_G)}{\omega_I^2 \tau_G}, \tag{11}$$

and

$$G_r = G_I'(1 - 2c_G \alpha_G \tau_G). \tag{12}$$

Table 1 shows the values that were obtained using these equations for a standard polymer used in ultrasonic transducer design. The remaining coefficients of the elastic modulus tensor are then given by $c_{12}^s = G(2G - Y)/(Y - 3G)$ and $c_{11}^s = c_{12}^s + 2G$.

4 Results

In order to gauge the effect that frequency dependent loss has on the operational characteristics of composite piezoelectric transducers a series of model simulations are now presented. In the first section the effect that frequency dependent loss in a standard polymer filler has on the transmission sensitivity, electrical impedance and electromechanical coupling coefficient is investigated.

4.1 A Hardset Passive Phase (HY1300/CY1301)

In this section a piezoelectric composite transducer composed of a hardset polymer filler material (see Table 1), a backing material (see Table 2) and a ceramic

Parameter	Symbol/Units	Value
Shear modulus (real part)	$G'(\text{kg m}^{-1}\text{s}^{-2})$	1.57×10^9
Young's modulus (real part)	$Y'(\text{kg m}^{-1}\text{s}^{-2})$	4.28×10^9
Shear Velocity	$c_G(\text{m s}^{-1})$	1.17×10^3
Longitudinal Velocity	$c_Y(\text{m s}^{-1})$	2.51×10^3
Density	ρ (kg m^{-3})	1.15×10^3
Dielectric constant	$\epsilon(-)$	4
Frequency of measurement	f_I (Hz)	5.00×10^5
$\tan\delta$ frequency maximum	$f_{max}(Hz)$	3.15×10^5
G Attenuation Coefficient	$\alpha_G^0(Np/m)$	41^b
Y Attenuation Coefficient	$\alpha_Y^0(Np/m)$	16^b
Calculated Values		
Unrelaxed shear modulus	$G_u(kgm^{-1}s^{-2})$	1.60×10^9
Relaxed shear modulus	$G_r(kgm^{-1}s^{-2})$	1.50×10^9
Shear relaxation time	$\tau_G(s)$	4.88×10^{-7}
Unrelaxed Young's modulus	$Y_u(kgm^{-1}s^{-2})$	4.35×10^9
Relaxed Young's modulus	$Y_r(kgm^{-1}s^{-2})$	4.11×10^9
Young's relaxation time	$\tau_Y(s)$	4.91×10^{-7}

Table 1: Physical properties of the polymer phase HY1300/CY1301 Hardset [9].

phase PZT5H (see Table 3) is investigated.

-	Constant	Units	Value
Transducer thickness	L	m	6×10^{-3}
Backing material impedance	Z_1	Rayls	2×10^6
Front material impedance	Z_2	Rayls	1.5×10^6

Table 2: Physical properties of the transducer

In Figure 1(a) the electrical impedance of the device, given by equation (1), is plotted as a function of the driving frequency. The effect of incorporating

frequency dependent loss into the model can be seen by comparing the no loss case (dashed line) with the loss case (full line). It can be seen that introducing loss for these materials has had very little effect on the profile except at the mechanical resonant frequency. Here there is a decrease of around ten percent in the magnitude of the electrical impedance although its frequency (the mechanical resonant frequency) remains constant. This reduction in amplitude gives rise to a ten percent increase in the bandwidth. In Figure 1(b) the associated transmission sensitivity, given by equation (2) is plotted. The addition of the elastic loss does not affect the profile except at the third harmonic whose peak value is reduced by ten percent.

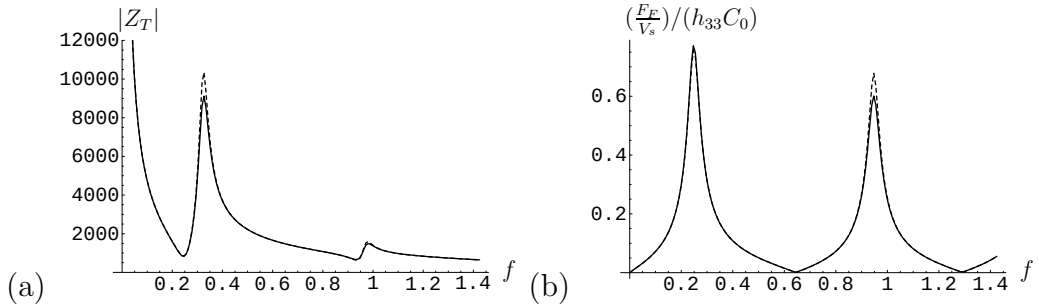

Figure 1: (a) Electrical impedance $|Z_T|$ (Ω) against frequency f (MHz), and (b) Transmission sensitivity (nondimensionalised) $(F_F/V_s)/(h_{33}C_0)$ against frequency f (MHz) for a 1-3 composite transducer with the hardset material HY1300/CY1301 (frequency dependent, elastic loss (full line), no loss (dashed line)).

In Figure 2 the electromechanical coupling coefficient, given by equation (4), is plotted as a function of the volume fraction of the ceramic phase (ψ). It can be seen that the frequency dependent loss reduces the efficiency across the full range of volume fractions. From a design perspective the highest efficiency (of around $k = 0.65$) occurs at a ceramic volume fraction of around $\psi = 0.6$. The diagram also highlights the benefits of using a composite design. The coefficient has risen by around 30 per cent from $k = 0.5$ for the pure ceramic ($\psi = 1$) to the optimum ceramic volume fraction of around $\psi = 0.6$.

In Figure 3(a) the reception sensitivity frequency profile, given by equation

-	Constant	Units	Value
elastic constant	c_{11}	Nm^{-2}	12.72×10^{10}
elastic constant	c_{12}	Nm^{-2}	8.02×10^{10}
elastic constant	c_{13}	Nm^{-2}	8.47×10^{10}
elastic constant	c_{33}	Nm^{-2}	11.74×10^{10}
dielectric constant	ϵ_{33}	-	1.70×10^{3}
dielectric constant	ϵ_{11}	-	1.47×10^{3}
Loss Tangent	$\tan\delta$	-	1/65
density	ρ_b	kg m^{-3}	7.50×10^{3}
Piezoelectric stress coefficient	e_{33}	C m^{-2}	23.30
Piezoelectric stress coefficient	e_{31}	C m^{-2}	-6.50

Table 3: Physical properties of the ceramic phase PZT5H [10].

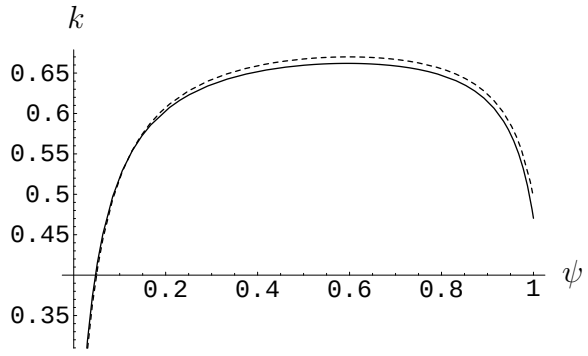

Figure 2: Electromechanical coupling coefficient k against ceramic volume fraction ψ for a 1-3 composite transducer with the hardset material HY1300/CY1301 with (a) frequency dependent, elastic loss (full line), and (b) no loss (dashed line) (at the electrical resonant frequency).

(3), is plotted against the ceramic volume fraction. As the ceramic volume fraction decreases the resonant frequencies also decrease. Since the mechanical impedance decreases as the volume fraction of the polymer increases, then the wave velocities decrease along with the associated resonant frequencies. It can also be seen that the magnitude of the reception sensitivity increases as the

polymer phase is slowly introduced to the pure ceramic ($\psi = 1$). In Figure 3(b) the electrical impedance frequency profile is plotted as a function of the ceramic volume fraction. Here it can be seen that an optimum profile (low amplitude at the electrical resonant frequency, high value at the mechanical resonant frequency) is achieved at an intermediate ceramic volume fraction. As the volume fraction diminishes the resonant behaviour ultimately vanishes and the device acts like a simple capacitor.

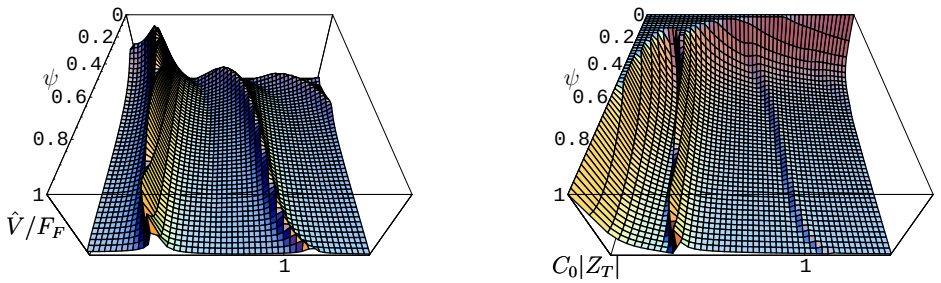

Figure 3: (a) Reception sensitivity (nondimensionalised) $\hat{V}/F_F = (V/F_F)(Z_c/(h_{33}C_0 b))$ against frequency f (MHz) and ceramic volume fraction ψ, and (b) Scaled electrical impedance $C_0|Z_T|$ (arbitrary units) against frequency f (MHz) and ceramic volume fraction ψ, for a 1-3 composite transducer with the hardset material HY1300/CY1301 and frequency dependent, elastic loss.

4.2 An Anisotropic Passive Phase

In this section the transmission and reception characteristics of a 1-3 composite transducer, with an anisotropic passive phase featuring high shear attenuation, are investigated; the shear attenuation in the supporting matrix is three orders of magnitude larger than in the previous section. One possible approach to realising such a material would be to use a high shear loss polymer phase embedded with spherical particles that are spatially aligned in linear columns. In the direction parallel to the ceramic pillars this alignment creates a striated effect whereas, perpendicular to this direction, the material consists of randomly arranged columns set in the supporting matrix. The frequency dependent elas-

tic loss for the Young's (Y) and shear (G) moduli are calculated independently for both the inclusions and the supporting matrix. Although the LSM is one-dimensional, the anisotropy in the passive phase does affect the calculation of the effective material properties, particularly because of the high shear attenuation. The effective properties of the passive phase are then calculated using mixing rules for parallel and series arrangements [11].

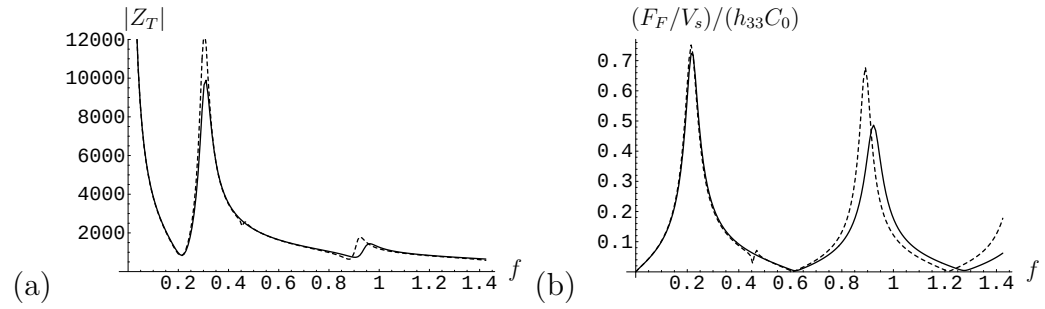

Figure 4: (a) Electrical impedance $|Z_T|(\Omega)$ against frequency f (MHz), and (b) Transmission sensitivity (nondimensionalised) $(F_F/V_s)/(h_{33}C_0)$ against frequency f (MHz), for an anisotropic passive phase, 1-3 composite transducer (frequency dependent loss (full line), no loss (dashed line)).

In Figure 4(a) the electrical impedance frequency profile for such a device is shown. Due to the high shear attenuation in this polymer there is a larger reduction in the impedance amplitude when the loss is included (around 25 percent). There is also a slight shift (around 5 percent) in the mechanical resonant frequency to a lower value. The transmission sensitivity frequency response in Figure 4(b) also shows a similar decrease in amplitude and a frequency shift. At this volume fraction of supporting matrix (the volume fraction of the supporting matrix is $\phi = 0.7$) the material has lower values for its moduli than the hardset material discussed in the previous section. However the anisotropy leads to a similar amplitude for the peak transmission sensitivity. This efficiency is also exhibited by the electromechanical coupling coefficient shown in Figure 5. The peak value of around $k = 0.73$ is achieved at a volume fraction of polymer of $\psi = 0.55$.

In Figure 6(a) the reception sensitivity frequency response is shown as a

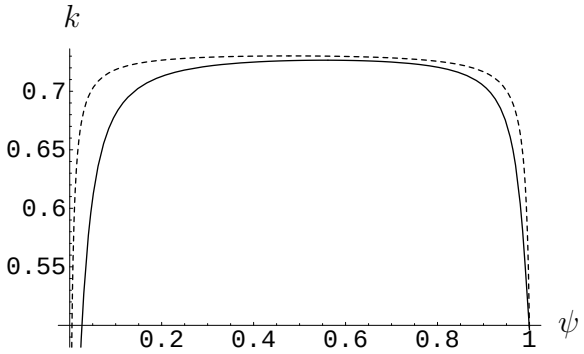

Figure 5: Electromechanical coupling coefficient k against the volume fraction of the ceramic phase ψ for an anisotropic passive phase, 1-3 composite transducer with (a) frequency dependent loss (full line), and (b) no loss (dashed line).

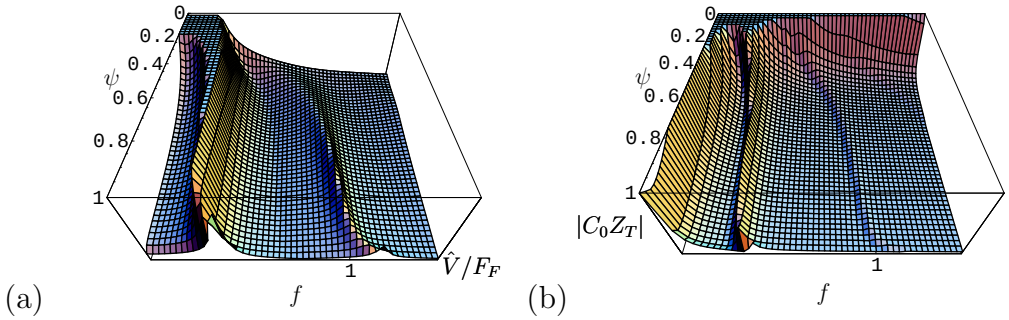

Figure 6: (a) Reception sensitivity (nondimensionalised) $\hat{V}/F_F = (V/F_F)(Z_c/(h_{33}C_0b))$ against frequency f (MHz) and ceramic volume fraction ψ, and (b) Scaled electrical impedance $|C_0Z_T|$ (arbitrary units) against frequency f (MHz) and ceramic volume fraction ψ, for an anisotropic passive phase, 1-3 composite transducer with frequency dependent loss.

function of the ceramic volume fraction. As before, the addition of the polymer serves to increase the amplitude of the main lobe. As the volume fraction of the ceramic decreases the main peak disappears and the device no longer displays the desired resonant behaviour.

4.3 Comparison to Finite Element Modelling

In Figure 7 the LSM is compared to FEM [12] by examining the impedance characteristics of a range of 2-2 composite transducers, all with thickness 3.8 ×

Parameter	Symbol/Units	Supporting Matrix	Inclusions
Shear modulus (real part)	$G'(kgm^{-1}s^{-2})$	4.00×10^8	2.00×10^9
Young's modulus (real part)	$Y'(kgm^{-1}s^{-2})$	1.10×10^9	5.00×10^9
$\tan\delta$ frequency maximum	$f_{max}(Hz)$	3.00×10^5	3.00×10^5
Frequency of Interest	$f_I(Hz)$	5.00×10^5	5.00×10^5
G Attenuation Coefficient	$\alpha_G^0(Np/m)$	2.00×10^4	100
Y Attenuation Coefficient	$\alpha_Y^0(Np/m)$	200	10
Density	$\rho\ (kgm^{-3})$	1.00×10^3	2.00×10^3
Dielectric constant	$\epsilon(-)$	2.4	1
Shear Velocity	$c_G(\text{m s}^{-1})$	6.32×10^2	1.00×10^3
Longitudinal Velocity	$c_Y(\text{m s}^{-1})$	1.05×10^3	1.58×10^3
Calculated Values			
Unrelaxed shear modulus	$G_u(kgm^{-1}s^{-2})$	3.57×10^{10}	2.08×10^9
Relaxed shear modulus	$G_r(kgm^{-1}s^{-2})$	1.07×10^8	1.80×10^9
Shear relaxation time	$\tau_G(s)$	2.90×10^{-8}	4.94×10^{-7}
Unrelaxed Young's modulus	$Y_u(kgm^{-1}s^{-2})$	1.20×10^9	5.03×10^9
Relaxed Young's modulus	$Y_r(kgm^{-1}s^{-2})$	8.89×10^8	4.92×10^9
Young's relaxation time	$\tau_Y(s)$	4.56×10^{-7}	5.24×10^{-7}

Table 4: Physical properties of an anisotropic passive phase.

10^{-3}m. Using the FEM to model a 1-3 composite structure requires a three dimensional model and this is computationally expensive. A 2-2 design however can be captured by a two dimensional FEM and this significantly decreases the computation times. A to D in Table 1 are specific examples of the high shear attenuation materials discussed in the previous section. For comparison purposes plot (a) shows the response when using the hardset polymer which has a low shear attenuation (see Table 1).

The oscillations in electrical impedance at the lower frequencies in plot(a) represent the undesirable low frequency modes which interfere with the piston-

Constant	Softset	Material A
G'(kg m^{-1}s^{-2})	6.50×10^8	3.38×10^8
Y'(kg m^{-1}s^{-2})	1.84×10^9	9.68×10^8
c_G(m s^{-1})	747	549
c_Y(m s^{-1})	2000	1605
ρ (kg m^{-3})	1.16×10^3	1.12×10^3
ϵ	4	4
α_G^0 (db/m)	6063	21281
α_Y^0 (db/m)	825	565
f_I (MHz)	0.5	0.5

Table 5: Physical properties of the passive phase materials.

Constant	Material B	Material C	Material D
G'(kg m^{-1}s^{-2})	2.76×10^8	2.304×10^8	4.35×10^8
Y'(kg m^{-1}s^{-2})	7.95×10^8	6.659×10^8	1.20×10^9
c_G(m s^{-1})	539	498	676
c_Y(m s^{-1})	1635	1584	1533
ρ (kg m^{-3})	0.95×10^3	0.93×10^3	0.95×10^3
ϵ	4	4	4
α_G^0 (db/m)	10388	10388	7062
α_Y^0 (db/m)	87	104	80
f_I (MHz)	0.5	0.5	0.5

Table 6: Physical properties of the passive phase materials.

like motion of the device. It is necessary to use a higher dimensional model, such as the FEM used here, to display these modes; the one-dimensional LSM method has a smooth impedance curve at these frequencies. The two methods do agree on the magnitude and trend of the curve in this low frequency region. However, the LSM prediction of the electrical impedance magnitude at the first peak (the

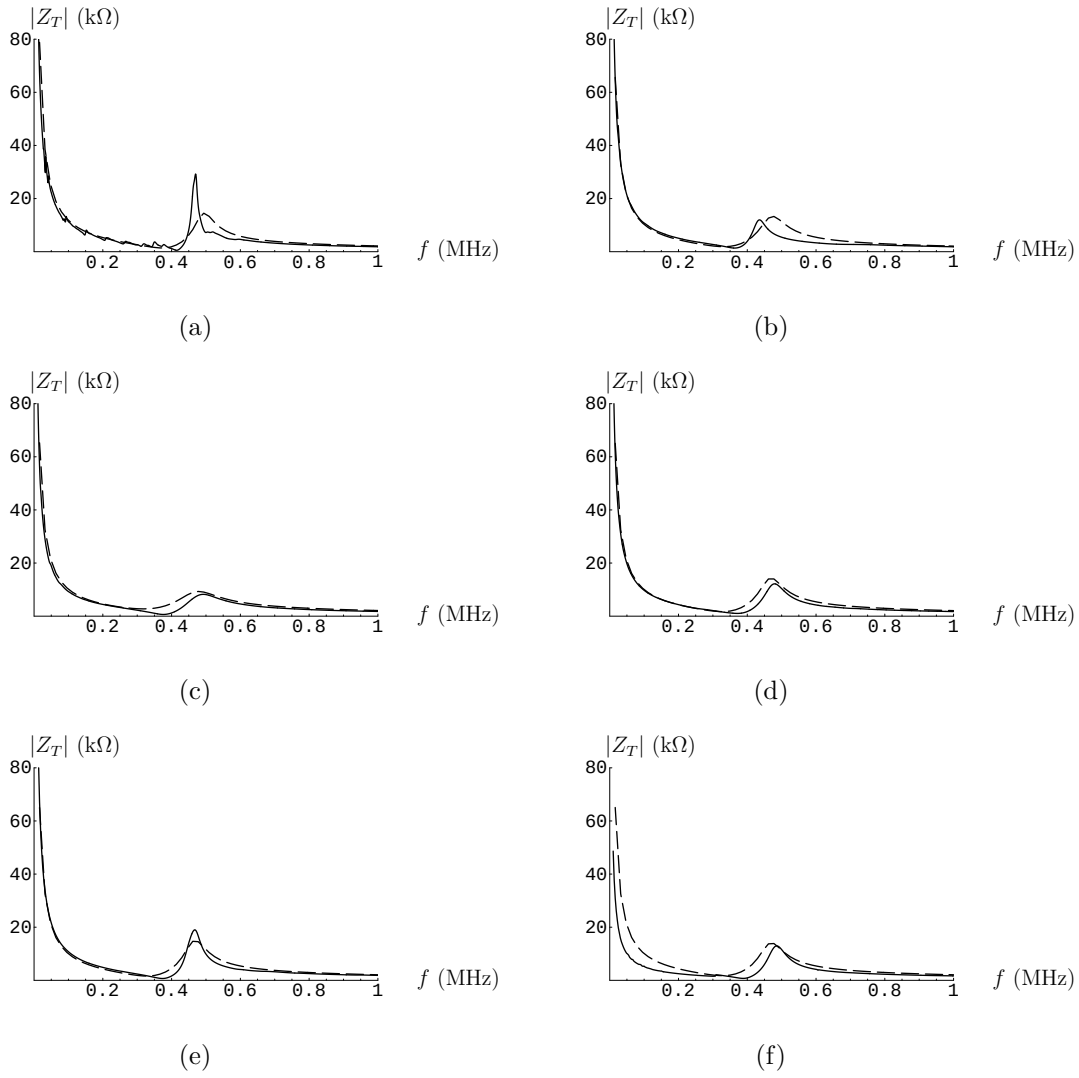

Figure 7: Electrical impedance characteristics for frequency dependent, elastic loss transducers with the passive phase materials described in Tables 5 and 6 using FEM (solid line) and LSM (dashed line) with polymer phase (a) hardset, (b) softset, (c) Material A, (d) Material B, (e) Material C and (f) Material D.

mechanical resonant frequency) is about double that given by the FEM, and a larger bandwidth (about a four-fold increase) results. The location of this peak is also slightly shifted (by about ten percent) to a higher frequency. In plot (b) a softset polymer filler is used which has high shear and longitudinal attenuation (see Table 5). This has damped out the unwanted, low frequency modes but there may well be a decoupling of the ceramic and polymer phases. This would subsequently inhibit its ability to transfer energy into the load medium

and this explains the drop in the peak electrical impedance that can be seen. Here there is better agreement between the two methods on the magnitude of the first peak impedance, although the frequency discrepancy remains. In plot (c) a material with a high shear attenuation (three orders of magnitude larger than the standard hardset filler) and a relatively low longitudinal attenuation (about two orders of magnitude smaller than the shear attenuation) is modelled (see Table 5, Material A). This material damps out the unwanted shear modes which propagate through the polymer whilst having sufficient stiffness in the thickness direction to remain in phase with the ceramic pillars. Both methods are in agreement over the form of the electrical impedance profile with the FEM approach predicting a far lower value (around 1 K Ω compared to 5 KΩ in the LSM case) at the electrical resonant frequency (i.e. the first minimum). Plots (d) and (e) show the electrical impedance curves for Materials B and C in Table 6. These materials are similar to Material A, having high shear attenuation and low longitudinal attenuation, although they are slightly less stiff (roughly a 20 percent reduction in the Young's and shear moduli) and the attenuation coefficients are smaller. Both plots show reasonable agreement between the two methods; the curves are almost identical away from the resonant peak, the frequency location of the peak is comparable but there is roughly a 20 percent discrepancy in the magnitude of the peak value and in its bandwidth. Material D has a reduced degree of attenuation from these materials but it is slightly stiffer (both the Young's and shear moduli are doubled, see Table 6). Although there is still good agreement between the two methods around the resonant mode, this is less true at the lower frequencies. The FEM predicts a lowering of the impedance in this range and this may well be due to some decoupling between the polymer and ceramic phases.

5 Conclusions

In this paper the linear systems model (LSM) of a 1-3 composite piezoelectric transducer is extended to incorporate frequency dependent elastic loss in the polymer phase. This facilitates a study of the effect of elastic loss in such polymers on the operating characteristics of these transducers. Composite transducers composed of a piezoelectric ceramic and a passive polymer phase provide better electromechanical coupling and acoustic impedance characteristics than conventional single phase transducers. Ideally a single longitudinal mode in the thickness direction will drive the transducer in a piston like fashion, however other parasitic modes, propagating in other directions, can interfere with this behaviour. Hence it is of interest to theoretically predict the design criteria that will provide a large frequency band gap between the desired thickness mode and these other waves. One possibility is to use polymers that are highly attenuative to shear waves in order to reduce the cross-talk between the ceramic pillars. Theoretical results regarding the operating characteristics of a device are reported for a range of passive phase materials including high shear attenuation materials.

A hypothetical material was proposed which is composed of spherical inclusions suspended in a softer supporting matrix. In the direction parallel to the ceramic pillars the inclusions are aligned to create a striated effect whereas, perpendicular to this direction, the material consists of randomly arranged columns set in the supporting matrix. Although the LSM is one-dimensional, the anisotropy in the passive phase does affect the calculation of the effective material properties, particularly because of the high shear attenuation. The effective properties of the passive phase were calculated using mixing rules for parallel and series arrangements. Due to the high shear attenuation in this polymer there was a reduction in the impedance amplitude and a shift in the mechanical resonant frequency to a lower value. The LSM model was then compared to a finite element model (FEM) by examining the impedance characteristics of a range of

high shear attenuation, 2-2 composite transducers. The two methods showed reasonable agreement in all the cases considered; the plots were almost identical away from the resonant peak, the frequency location of the peaks were comparable but there was in some cases a 20 percent discrepancy in the magnitude of the peak value and in its bandwidth. The FEM showed that the use of a high shear attenuation polymer damps out the unwanted, low frequency modes whilst maintaining a reasonable impedance magnitude.

References

[1] G. Hayward and J.A. Hossack, "Unidimensional Modelling of 1-3 Composite Transducers.", *JASA*, Vol. 88, No. 2, pp. 599-607, (1990).

[2] G. Hayward, "A systems feedback representation of piezoelectric transducer operational impedance.", *Ultrasonics*, Vol. 22, No. 4, pp. 153-162, (1984).

[3] G. Hayward, C.J. MacLeod and T.S. Durrani, "A Systems Model of the Thickness Mode Piezoelectric Transducer.", *JASA*, Vol. 76, No.2, pp. 369-382, (1984).

[4] G. Hayward, "The influence of pulser parameters on the transmission response of piezoelectric transducers.", *Ultrasonics*, Vol. 23, No. 3, pp. 103-112, (1985).

[5] G. Hayward, "Using a block diagram approach for the evaluation of electrical loading effects on piezoelectric reception.", *Ultrasonics*, Vol. 24, No. 3, pp. 156-164, (1986).

[6] W.A. Smith and B.A. Auld, "Modelling 1-3 Composite Piezoelectrics: Thickness-Mode Oscillations.", *IEEE Trans UFFC*, Vol. 38, No. 1, pp. 40-47, (1991).

[7] N.G. McCrum, B.E. Read and G. Williams, *Anelastic and Dielectric Effects in Polymeric Solids*, John Wiley and Sons, (1967).

[8] R.S. Lakes, *Viscoelastic Solids*, CRC Press, London, (1999).

[9] R.L. O'Leary, G. Smillie, G. Hayward and A.C.S. Parr, *CUE Materials Database*, Technical Report, Centre for Ultrasonic Engineering, University of Strathclyde, Glasgow, Scotland, (2002), *www.cue.ac.uk*.

[10] Ferroperm UK Ltd, Vauxhall Industrial Estate, Ruabon, Wrexham, United Kingdom, LL14 6HA.

[11] S.S. Abramchuk, I.P. Dimitrienko and V.N. Kiselev, "Calculation of the Elastic Characteristics of a Unidirectional Fiber Composite by the Cross-Section Method.", *Mech. Composite Mat.*, Vol. 18, No. 6, pp. 641-647.

[12] *PZFLEX*, Weidlinger Associates, 4410 El Camino Real, Los Altos, CA 94022.